Korean J. Chem. Eng., 34(8), 2198-2203 (2017)
DOI: 10.1007/s11814-017-0130-1

pISSN: 0256-1115
eISSN: 1975-7220

Hydrogen production from biomass: The behavior of impurities over a CO shift unit and a biodiesel scrubber used as a gas treatment stage

Jürgen Loipersböck*,†, Marco Lenzi*, Reinhard Rauch*,*, and Hermann Hofbauer****

*Bioenergy2020+ GmbH, Wienerstraße 49, 7540 Güssing, Austria
**TU Wien, Institute of Chemical Engineering, Getreidemarkt 9/166, 1060 Vienna, Austria
***Karlsruher Institut für Technologie, 76021 Karlsruhe, Germany
(*Received 1 February 2017 • accepted 11 May 2017*)

Abstract−Most of the hydrogen produced is derived from fossil fuels. Bioenergy2020+ and TU Wien have been working on hydrogen production from biomass since 2009. A pilot plant for hydrogen production from lignocellulosic feedstock was installed onsite using a fluidized bed biomass gasifier in Güssing, Austria. In this work, the behavior of impurities over the gas conditioning stage was investigated. Stable CO conversion and hydration of sulfur components could be observed. Ammonia, benzene, toluene, xylene (BTX) and sulfur reduction could be measured after the biodiesel scrubber. The results show the possibility of using a commercial Fe/Cr-based CO shift catalyst in impurity-rich gas applications. In addition to hydrogen production, the gas treatment setup seems to also be a promising method for adjusting the H_2 to CO ratio for synthesis gas applications.

Keywords: Hydrogen, CO Shift, Biodiesel Scrubber, Catalyst Poisoning, Gas Conditioning

INTRODUCTION

Human dependence on fossil fuels has led to several economic and environmental crises. By 2020, the European Union (EU) aims to have 10% of the transport fuel consumption of each EU country coming from renewable sources, such as biofuels [1]. Thus, renewable hydrogen has been investigated as one possible source to replace hydrogen from fossil fuels. H_2 is required for ammonia and methanol synthesis, as well as in refineries and for energetic purposes [2-7]. In 2007, the worldwide hydrogen demand was about 65 million tons, with a growing tendency caused by the greater amounts needed for the hydrotreatment of heavier raw oil fractions [8]. A total of 96% of the hydrogen production from 2014 was based on fossil fuels, with natural gas being the main supplier (49%) [9].

Hydrogen can be produced by several technologies, including gasification and hydrogen separation from lignocellulosic feedstock. To obtain more information about hydrogen production based on steam gasification, a flow chart for a demonstration plant on the scale of a 50 MW fuel input, producing 10,000 Nm^3/h of hydrogen, was developed [10]. For this demo plant, the mass and energy balances were calculated, and based on these data a cost estimation was performed.

To verify the proper function of such a hydrogen production plant, based on biomass-derived feedstock, a pilot plant onsite at the combined heat and power plant CHP Güssing was built, where a dual fluidized bed (DFB) steam blown gasifier is in operation. From this gasifier, a slip stream of 5 Nm^3/h (dry) product gas was taken and used for the pilot plant. Table 1 shows the typical gas composition of the product gas.

Fig. 1 shows a flow sheet of the hydrogen production plant. The plant consists of a DFB to produce a high caloric product gas, a

Table 1. Typical composition of product gas from biomass steam gasification in Güssing, Austria [11,12]

H_2O	35-45 vol-%	H_2S	150-200 ppm (dry)
CH_4	8-12 vol-% (dry)	COS	5-9 ppm (dry)
C_2H_4	2-3.5 vol-% (dry)	Thiophene	20-25 ppm (dry)
C_2H_6	0.1-0.3 vol-% (dry)	Mercaptane	1-10 ppm (dry)
C_3 fraction	0.5-0.7 vol-% (dry)	Tar	2-5 g/Nm^3 (dry)
CO	20-30 vol-% (dry)	BTX	15-20 g/Nm^3 (dry)
CO_2	15-25 vol-% (dry)	NH_3	1000-2000 ppm (dry)
H_2	35-45 vol-% (dry)	HCN	5-30 ppm (dry)
N_2	1-3 vol-% (dry)	LHV	12.9-13.6 MJ/Nm^3 (dry)

†To whom correspondence should be addressed.
E-mail: juergen.loipersboeck@bioenergy2020.eu
‡5th International Conference on Gasification and Its Application.

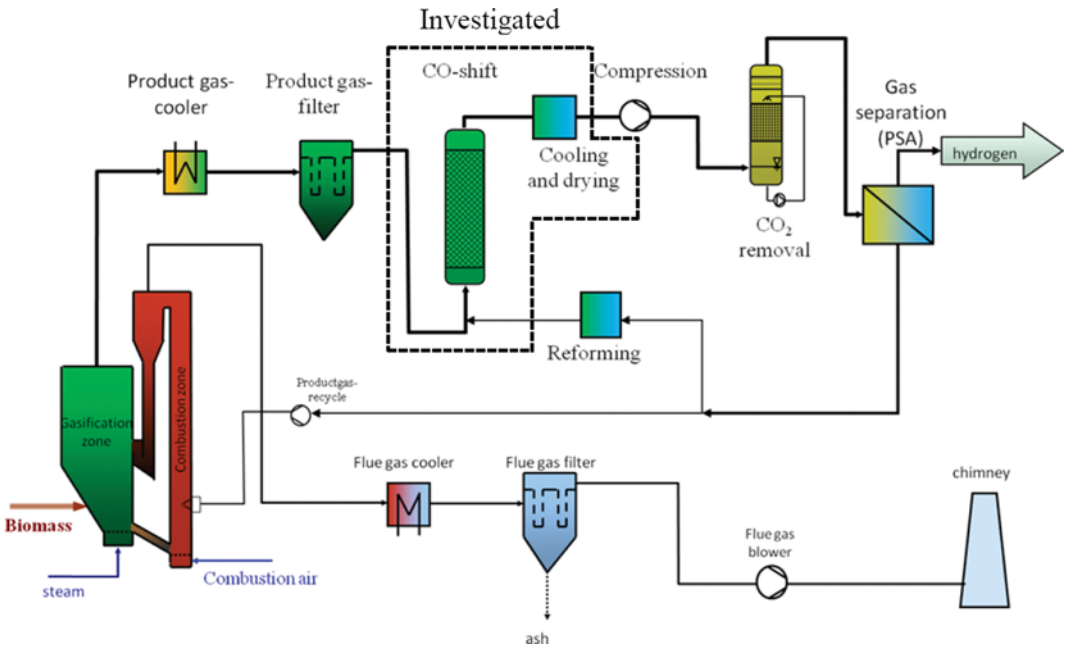

Fig. 1. Flow sheet of the hydrogen production plant.

product gas cooler, a bag house filter to remove dust particles, a CO shift stage to enhance the hydrogen output and an organic solvent scrubber to remove water and tar from the product gas. Next, the process steps include compression of the product gas, a CO_2 removal stage to separate sour gas components, pressure swing adsorption used as a hydrogen purification unit and a steam reformer to enhance the efficiency of the plant. With this plant setup, chemical efficiencies of over 60% (based on net calorific values) and total efficiencies of up to 80% can be reached by the utilization of waste heat [13].

To improve the quality of product gas, a CO shift stage and a biodiesel scrubber were used to increase the hydrogen yield, lower carbon monoxide production and to decrease impurities that may cause problems for further process steps of hydrogen production [14,15].

Typical CO shift catalysts can be divided into high temperature and low temperature systems. In this study, high temperature catalysts for use in sulfur containing gas were investigated. For high temperature shift catalysts, iron/chromium- and cobalt/molybdenum-based materials are common. Fe/Cr catalysts perform well up to concentrations of 200-250 ppm H_2S, while Co/Mo-based catalysts require hydrogen sulfide concentrations of at least 100 ppm [11,16-18]. Typically, high temperature CO shift stages are operated adiabatically at space velocities from 400 to 2,000 h^{-1} and temperatures of 350 to 550 °C at the inlet [8].

This work focuses on the behavior and influence of impurities on a hydrogen production process, as seen in Fig. 1. The product gas was extracted from the DFB gasifier after dust removal. Tar and water were removed after the CO shift by a biodiesel scrubber.

MATERIALS AND METHODS

1. CHP Güssing

CHP Güssing produces a high quality product gas by using a DFB steam blown gasifier. The major components of this product gas are hydrogen, carbon monoxide, carbon dioxide and methane (see Table 1). The basic principles of DFB gasification technology are shown in Fig. 2.

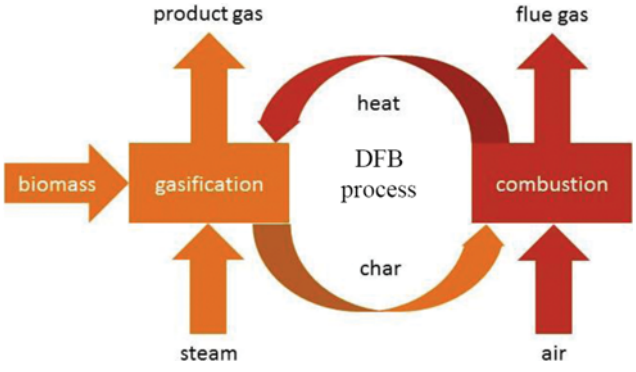

Fig. 2. Basic principles of the DFB process [19].

The DFB process consists of two reaction chambers: the gasification zone and the combustion zone. In the gasification zone, steam is used for fluidization and a hot bed material delivers the heat for the gasification reactions of the lignocellulosic feedstock.

The combustion zone is operated with air and combustion of non-gasified carbon (char) takes place, which is transported from the gasification zone into the combustion zone. Product gas can be used as additional fuel to control the process temperatures.

The heat required for the steam gasification reactions is transported by the bed material from the exothermic combustion chamber into the endothermic gasification chamber. Generated by the two reaction chambers, which are coupled due to the bed material, the resulting gasification product is an almost nitrogen-free gas that is well suited for synthesis applications or hydrogen production. The

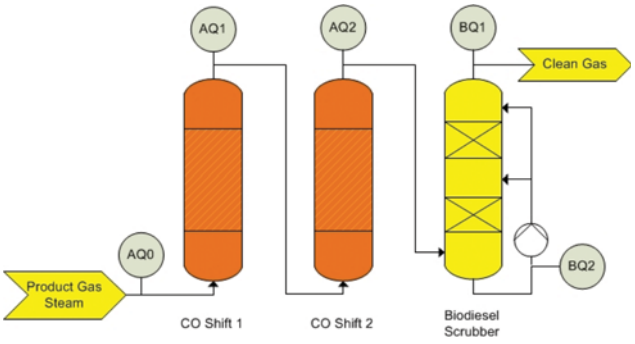

Fig. 3. Flow scheme of CO shift and biodiesel scrubber.

dust in the gas is removed by a filter, resulting in a dust-free, hydrogen-rich synthesis gas. This synthesis gas was used as feed gas for the research activities presented in this study.

2. CO Shift and Biodiesel Scrubber

The CO shift unit is the first process step of the pilot plant. Directly after the product gas filter of the CHP, a slipstream of product gas (Table 1) is taken. The main components of this gas are CO, CO_2, H_2, CH_4 and steam. In the CO shift stage, the carbon monoxide content is reduced. Therefore, two reactors with a different height/diameter ratio were designed to test the behavior of the catalyst using different space velocities and temperatures. The CO shift stage was designed for atmospheric pressure. The main reaction in the CO shift unit is shown in Eq. (1). The main reaction has an exothermic behavior and the CO shift reactors are operated as adiabatic reactors.

$$CO+H_2O \rightarrow CO_2+H_2 \quad \Delta H_R^0\,(298\,K) = -40.6\,kJ/mol \tag{1}$$

Fig. 3 shows a scheme of the pilot plant consisting of two CO shift reactors and a biodiesel scrubber. The product gas of the CHP is taken at 150 °C and carried to the pre-heating step of CO-shift reactor 1, where the gas is heated from 150 °C to a maximum temperature of 400 °C. The entrance temperature in the catalyst bed of CO shift reactor 1 is measured with a thermocouple (type J). Along the catalyst bed, another four thermocouples measure the bed temperature. Another thermocouple is used to measure the outlet gas temperature of CO shift reactor 1. The tail gas of reactor 1 is heated to the desired inlet temperature of CO shift reactor 2. Thus, reactor 2 has a lower height/diameter ratio and there are fewer thermocouples in the catalyst bed. The inlet and outlet temperatures of reactor 2 are measured with two thermocouples. Three thermocouples are placed along the bed. In total, the two reactors have 24 thermocouples for temperature measurement and control.

Additional water can be added before the CO shift to adjust the steam/carbon ratio. Gas samples are taken at the sample points AQ0, AQ1 and AQ2. Three pressure transmitters are used to measure the pressure drop over the first and second reactors. After the two CO shift stages, the gas is sent to a biodiesel scrubber for tar removal and cooling.

After the CO shift process, the gas is rich in hydrogen but still contains tar and water. In a biodiesel scrubber, components like tar, water and ammonia can be removed effectively. Fig. 3 shows the flow scheme of the biodiesel scrubber. As a solvent, rapeseed methyl ester, which yields excellent results for tar and water removal [12], was used. Through a two staged cooling process, the water content can be minimized to 3-5%. In the first stage, temperatures of 10-30 °C are common. The second stage is used to cool the tail gas to 3-10 °C. A continuous supply of fresh biodiesel and a blow down of used biodiesel was applied. For the flow measurement of biodiesel, floaters were used. Gas flow was measured by an orifice plate meter. Gas samples were taken at BQ1 and samples of the biodiesel were taken at BQ2.

3. Analytics and Sampling

The composition of the product gas was determined by measurements with a gas chromatograph (GC) Clarus 500 from Perkin Elmer. The GC was equipped with three different columns, connected with two automated valves and an injection loop of 500 µl. Two types of detectors were used: a thermal conductivity detector (TCD) for permanent gases (O_2, N_2, CO and CO_2) and a flame ionization detector (FID) for hydrocarbons (CH_4, C_2H_6, C_2H_4, C_3H_8 and C_3H_6). The synthesis gas to be analyzed was first entered in one Porapak column for a pre-separation. After this, CO_2 and the hydrocarbons larger than CH_4 were sent to the second Porapak column, while O_2, H_2, N_2, CO and CH_4 were led to the third column, a molecular sieve. The components were then detected by the TCD at 200 °C and FID at 300 °C [20]. The hydrogen concentration was calculated as 100 minus the sum of the gas concentration given by the two detectors. The detection limit was 500 v-ppm. The maximum error of the GC is 5% of the measured value (relative). As carrier gases, (A) 23 ml/min of helium 5.0 and (B) 30 ml/min of helium 5.0 were used. Calibration was realized with a calibration gas with seven components. For sampling, gas was drained through an impinger bottle filled with biodiesel and sent into a sample bag. This sample bag was used for GC analysis.

Online gas detection was performed with a five-component gas analyzer. A continuous Magnos 206 oxygen analyzer, with a measurement range of 0-5% O_2 was used. For the measurement of carbon monoxide (0-40%), carbon dioxide (0-40%) and methane (0-100%), an infrared photometer (Uras 26) was applied. Hydrogen (0-100%) was measured with a heat conductibility detector (Caldos 27).

Sulfur components were detected by using a GC (Perkin Elmer Clarus 500). A metal capillary column with an inner diameter of 0.32 mm (df 0.4 µm) and a length of 30 m was used to split the sulfur components in an oven through different interactions between the gas and column. A sulfur chemiluminescence detector was used to detect the sulfur components. The calibrated components were H_2S, COS, CH_4S, C_2H_6S, $C_4H_{10}S$, C_4H_8S, C_4H_4S and $(CH_3)_2S$. The maximum error of the GC is 5% of the measured value (relative). The detection limit was 10 ppb. The sampling for the sulfur analysis was completed with sample bags under hot conditions.

Ammonia sampling in the gas stream was carried out by absorption in a liquid. The product gas was drawn over impinger bottles filled with 1 M sulfuric acid. In the impinger bottles, an absorption process between NH_3 and sulfuric acid takes place. The NH_3 and sulfuric acid react to form ammonia sulfate. The total amount of gas drawn over the impinger bottles was measured in a gas meter at atmospheric pressure. The temperature was measured in the gas meter to calculate the volume at standard conditions. The time of

the sampling was also measured. This sorption solution was analyzed with an ion chromatograph. The maximum error of this method is 5% of the measured value (relative). Ammonia was analyzed by an external laboratory.

BTX analysis involved a Clarus 500 GC. For the column, a Restek MXT-1 (dimethyl polysiloxane) with a length of 60 m and an inner diameter of 0.53 mm was used. The coating thickness of the column was 0.25 μm df. Helium 5.0 was used as a carrier gas, with a flow of 4 ml/min. The heating procedure of the oven was adjusted to a heating up process where a temperature of 50 °C was held for 480 s. Then, a heating rate of 10 °C per min was adjusted until 200 °C was reached. This temperature was held for 300 s. An FID was used for detection. A single point calibration with a mixture of benzene (5.79 g/m^3), toluene (1.026 g/m^3) and three xylene isomers (0.192 g/m^3, 0.195 g/m^3 and 0.2 g/m^3) was applied. The maximum error of the GC was 10% of the measured value (relative). The sampling for the BTX analyses was completed with sample bags under hot conditions.

The sampled emulsion from the scrubber blowdown (BQ2) was analyzed for biodiesel and water content, with a separating funnel used to calculate the water content of the tail gas from the water gas shift. The water phase was analyzed for ammonia determination. In addition, a pH value measurement was carried out.

RESULTS AND DISCUSSION

1. Pilot Plant Operation

Stable plant operation could be achieved and no shutdowns were necessary during the experiments. During the whole test run, standard parameters, which were investigated in a previous parameter variation study by Chianese et al., were used [11]. Table 2 shows the elemental analysis of the biomass that was used during the test run.

Table 2. C, H, N, S analysis of the biomass used for the test run

	Content [m-%]
Carbon	48.73±0.34
Hydrogen	6.27±0.12
Nitrogen	0.27±0.04
Sulphur	0.46±0.09

Table 3 shows the measured process data together with the standard deviation.

A dry gas space velocity (based on the outlet flow) of 999 h^{-1} (±37.7 h^{-1}) was adjusted. A stable CO concentration of 4.14% (±0.19%) at the outlet of the biodiesel scrubber was measured, which resulted in a CO conversion of 77%. A total of 120 samples of sulfur, ammonia, hydrocyanic acid, gas and BTX were taken in 100 h of operation.

Table 4 shows the average concentration of sulfur and ammonia before CO shift reactor 1 (AQ0), after CO shift reactor 1 (AQ1), after CO shift reactor 2 (AQ2) and after the biodiesel scrubber.

With the measured data, mass balances were established to recalculate the flow of impurities over the water gas shift stage and the biodiesel scrubber.

2. Sulfur

H_2S was determined as the main sulfur component. As H_2S may influence the CO shift catalyst, a detailed investigation of the CO conversion and sulfur adsorption of the catalyst was carried out. Fig. 4 depicts the sulfur adsorption of the catalyst and the CO conversion dependency on the operation time. The sulfur adsorption rate of the CO shift catalyst is defined in Eq. (2).

$$\text{Sulfur adsorption rate} = \frac{\Sigma S_{in,\ CO\ shift} - \Sigma S_{out,\ CO\ shift}}{\Sigma S_{in,\ CO\ shift}} \quad (2)$$

Table 3. Process data from the CO shift stage and biodiesel scrubber

Water content	45.7%±%
CO concentration inlet	21.2%±1.3%
Inlet temperature CO shift reactor 1	382 °C±5.2 °C
Outlet temperature CO shift reactor 2	440 °C±7.3 °C
Inlet temperature CO shift reactor 2	422 °C±1.7 °C
Outlet temperature CO shift reactor 2	441 °C±1.7 °C
Space velocity (over sum of reactors)	999 h^{-1}±37.7 h^{-1}
Biodiesel supply	9 *l*/h±0.5 *l*/h
Biodiesel circulation bottom	400 *l*/h±12 *l*/h
Biodiesel temperature bottom	10.7 °C±1.2 °C
Biodiesel circulation top	296 *l*/h±11 *l*/h
Biodiesel temperature top	7.1 °C±0.8 °C
CO concentration outlet biodiesel scrubber	4.14%±0.19%

Table 4. Average concentrations of sulfur and ammonia over the water gas shift stage and RME scrubber

	AQ0	AQ1	AQ2	BQ1
H_2S [ppm]	167±15	118±43	99±45	93±45
COS [ppm]	7.1±0.6	2.8±0.3	1.5±0.7	1.3±0.8
Thiophene [ppm]	23±2.0	21±2.7	22±1.7	6.4±1.5
Mercaptanes [ppb]	112±23	899±420	BDL	BDL
Dimethylsulfide [ppb]	25±23	BDL	BDL	BDL
NH_3 [ppm]	3560±341	3246±433	2970±518	11.7±9.1
Benzene [g/Nm^3]	15±0.6	13±0.9	13±0.9	4.6±1.1
Toluene [g/Nm^3]	3.1±0.1	2.7±0.3	2.5±0.8	0.4±0.1
Xylene [g/Nm^3]	1.1±0.1	0.9±0.1	0.75±0.2	BDL

BDL=below detection limit

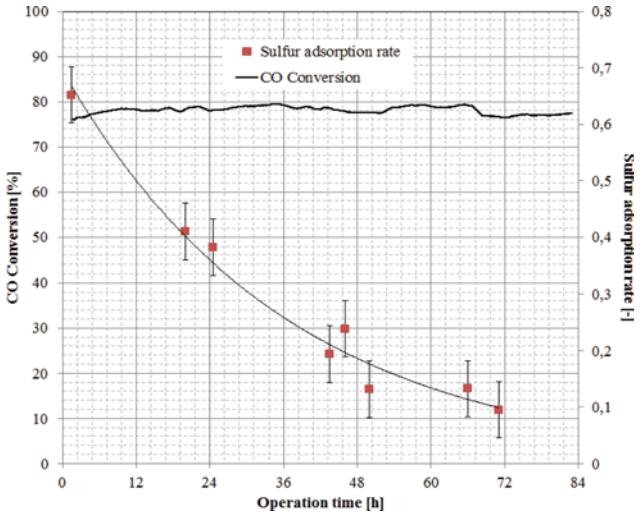

Fig. 4. Sulfur adsorption at the catalyst and CO conversion dependence on operation time.

It could be observed that H_2S concentration in the range of 150 to 200 ppm (Table 2) did not influence the CO conversion, which fluctuated between 75% and 80%.

At the start, sulfur adsorption rates of up to 65% could be measured. After 72 h of pilot plant operation, the H_2S adsorption of the catalyst was reduced to 10%. No dependency between CO conversion and sulfidation of the catalyst could be observed. Similar effects have been reported in the literature for long-term tests with lower sulfur loads [7,21].

In addition, stable CO conversion in the presence of H_2S containing gas and a conversion of sulfur components could be observed over the water gas shift stage. As the mass balance showed, methylmercaptan, ethylmercaptan, dimethylsulfide and carbonylsulfide were hydrated according to Eqs. (3)-(6).

$$COS+H_2O \leftrightarrow H_2S+CO_2 \quad (3)$$

$$COS+H_2 \leftrightarrow H_2S+CO \quad (4)$$

$$CH_4S+H_2 \leftrightarrow CH_4+H_2S \quad (5)$$

$$C_2H_6S+H_2 \leftrightarrow C_2H_6+H_2S \quad (6)$$

$$(CH_3)_2S+2H_2 \leftrightarrow 2CH_4+H_2S \quad (7)$$

Dimethylsulfide was fully hydrated in the first CO shift reactor, while an increase of mercaptanes could be observed. In the second CO shift reactor, these mercaptanes were fully hydrated. Carbonylsulfide was partially hydrated (68%), as indicated in Table 4.

In the biodiesel scrubber, a reduction of organic sulfur (e.g., thiophene) could be observed. Thiophene could be removed (70%) by biodiesel at the operation conditions described above. The effects on other sulfur components could not be detected. The effects of sulfur load on an iron/chromium-based water gas shift catalyst have been investigated by Chianese et al. [11]. A decrease in CO conversion could be observed when the H_2S concentration was increased.

3. Ammonia

An ammonia balance over the water gas shift reactors and biodiesel scrubber was performed. As indicated in Fig. 5, ammonia is not affected by the CO shift stage. A significant ammonia reduction of 99.7% over the biodiesel scrubber was measured. Due to the low temperatures in the biodiesel scrubber, water was condensed and ammonia dissolved in this phase.

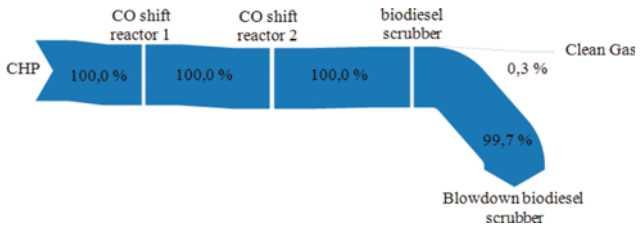

Fig. 5. Ammonia balance for water gas shift stage and biodiesel scrubber.

At the inlet of the pilot plant, an ammonia content of 11.55 g/h could be observed. Over the CO shift reactors, no significant change of the ammonia stream was detected. By biodiesel scrubbing and water condensation, the ammonia stream that was sent to the next plant stage could be reduced to 0.04 g/h. An amount of 11.54 g/h could be found in the blowdown water of the biodiesel scrubber.

The achieved results agreed with the literature, where ammonia was measured in a similar plant configuration. Fail et al. described a nearly constant NH_3 concentration over the water gas shift stage [7]. The decomposition of ammonia could not be observed. In the biodiesel scrubber, ammonia was removed nearly completely to 0.3% of the inlet concentration, which matches again with literature, where partwise ammonia reduction could be observed at higher scrubber temperatures [12]. An ammonia concentration in the range of 2,000-5,000 ppm seems to have no effect on the CO conversion.

4. BTX

Significant BTX reduction over the CO shift unit, apart from dilution effects, could not be observed. Only a slight reduction of toluene and xylene could be observed over the CO shift reactors (Table 3). Benzene was not affected, as a result of its stable ring structure. The main removal occurred in the RME scrubber. This treatment stage reached a BTX reduction of 70%. Higher hydrocarbons, like GC-MS or gravimetric tars, were not analyzed in this work, and will be investigated in a separate study. According to comparable studies, higher hydrocarbons (gravimetric, GC/MS tars) are hydrated over the CO shift stage, which results in easier removal by the RME scrubber.

CONCLUSIONS

A detailed study of the behavior of impurities over a gas cleaning step for hydrogen production by stem gasification has been presented. It could be proven that in a sulfur-rich atmosphere, an iron/chromium catalyst can be applied. A total CO conversion of 77% could be obtained. Process poisons, like ammonia, could be removed in the gas treatment stage. Sulfur components were partly removed or converted to H_2S. BTX could be removed up to 70%. For product gas synthesis applications, a temperature swing adsorption for additional sulfur and BTX removal will be used. The obtained data are crucial for the next larger design step.

OUTLOOK

For future research, further optimization of the pilot plant is recommended. Experiments with no additional water dosing and lower feedstock quality should be carried out. Also, an operation of the whole process chain should be completed.

ACKNOWLEDGEMENTS

This work was carried out within the framework of Bioenergy 2020+ GmbH. Bioenergy2020+ is funded by the states of Burgenland, Niederösterreich and Steiermark within the Austrian COMET program, managed by the research promotion agency Austria (FFG). This project received funding from the European Union's Horizon 2020 research and innovation program under grant agreement No. 680395.

The authors thank the project partners for the support during the execution of the project.

REFERENCES

1. European Commission, Energy 2020, *A strategy for competitive, sustainable secure energy,* Brussels (2010).
2. J.-F. Brau and M. Morandin, *Int. J. Hydrogen Energy*, **39**, 2531 (2014).
3. M. Farniae, M. Abbasi, A. Rasoolzadeh and M. R. Rahimpour, *J. Nat. Gas Sci. Eng.*, **14**, 158 (2013).
4. R. Rauch, A. Kiennemann and A. Sauciuc, *The Role of Catalysis for the Sustainable Production of Biofuels and Bio-chemicals*, Elsevier, Amsterdam (2010).
5. T. Li, H. Wang, Y. Yang, H. Xiang and Y. Li, *Fuel Process. Technol.*, **118**, 117 (2014).
6. S. Shao, A.-W. Shi, C. L. Liu, R.-Z. Yang and W.-S. Dong, *Fuel Process. Technol.*, **125**, 1 (2014).
7. S. Fail, N. Diaz, F. Benedikt, M. Kraussler, J. Hinteregger, K. Bosch, M. Hackel, R. Rauch and H. Hofbauer, *ACS Sustainable Chem. Eng.*, **2** , 2690 (2014).
8. K. Liu, C. Song and V. Subramani, *Hydrogen and Syngas Production and Purification Technologies*, John Wiley & Sons, New York (2009).
9. IEA, Hydrogen Production and Distribution, Paris (2007).
10. S. Müller, M. Stidl, T. Pröll, R. Rauch and H. Hofbauer, *Biomass Convers. Biorefin.*, **1**, 55 (2011).
11. S. Chianese J. Loipersböck, M. Malits, R. Rauch, H. Hofbauer, A. Molino and D. Musmarra, *Fuel Process. Technol.*, **132**, 39 (2015).
12. T. Pröll, I. Siefert, A. Friedl and H. Hofbauer, *Ind. Eng. Chem. Res.*, **44**, 1576 (2005).
13. K. Zech, E. Grasemann, K. Oehmichen, I. Kiendl, R. Schmersahl, S. Rönsch, M. Seiffert, F.Müller-Langer, W. Weindorf, S. Funke, J. Michaelis and M. Wietschel, Hy-NOW Evaluierung der Verfahren und Technologien für die Bereitstellung von Wasserstoff auf Basis von Biomasse, DBFZ, Leipzig (2013).
14. M. Laniecki and M. Ignacik, *Catal. Today*, **116**, 400 (2006).
15. K. Klier, *Catal. Today*, **15**, 361 (1992).
16. R. Hakkarainen, T. Salmi and R. L. Keiski, *Appl. Catal. A*, **99**, 195 (1993).
17. C. Ratnasamy and J. Wagner, *Catal. Rev. Sci. Eng.*, **51**, 325 (2009).
18. C. Hulteberg, *Int. J. Hydrogen Energy*, **37**, 3978 (2012).
19. M. Bolhàr-Nordenkampf, R. Rauch, K. Bosch, C. Aichernig and H. Hofbauer, *2nd Regional Conference on Energy Technology Towards a Clean Environment*, Phuket (2002).
20. A. Sauciuc, Z. Abosteif, G. Weber, A. Potetz, R. Rauch, H. Hofbauer, G. Schaub and L. Dumitrescu, *Biomass Convers. Biorefin.*, **2**, 253 (2012).
21. M. Kraussler, M. Binder and H. Hofbauer, *Int. J. Hydrogen Energy*, **41**, 6171 (2016).